Revised version (changes highlighted in blue)

Supplemental Information

- **Supplemental Figures S1-6**
- **Supplemental Figure Legends**
- **Supplemental Experimental Procedures**
- **Supplemental References**
- **Supplemental Table S1, related to Figure 1**
- **Supplemental Table S2, related to Figures 1 and 2**
- **Supplemental Table S3, related to Figure 1**
- **Supplemental Table S4, related to Figure 1**
- **Supplemental Table S5, related to Figures 2, 3, 4 and 5**
- **Supplemental Table S6, related to Figure 6**

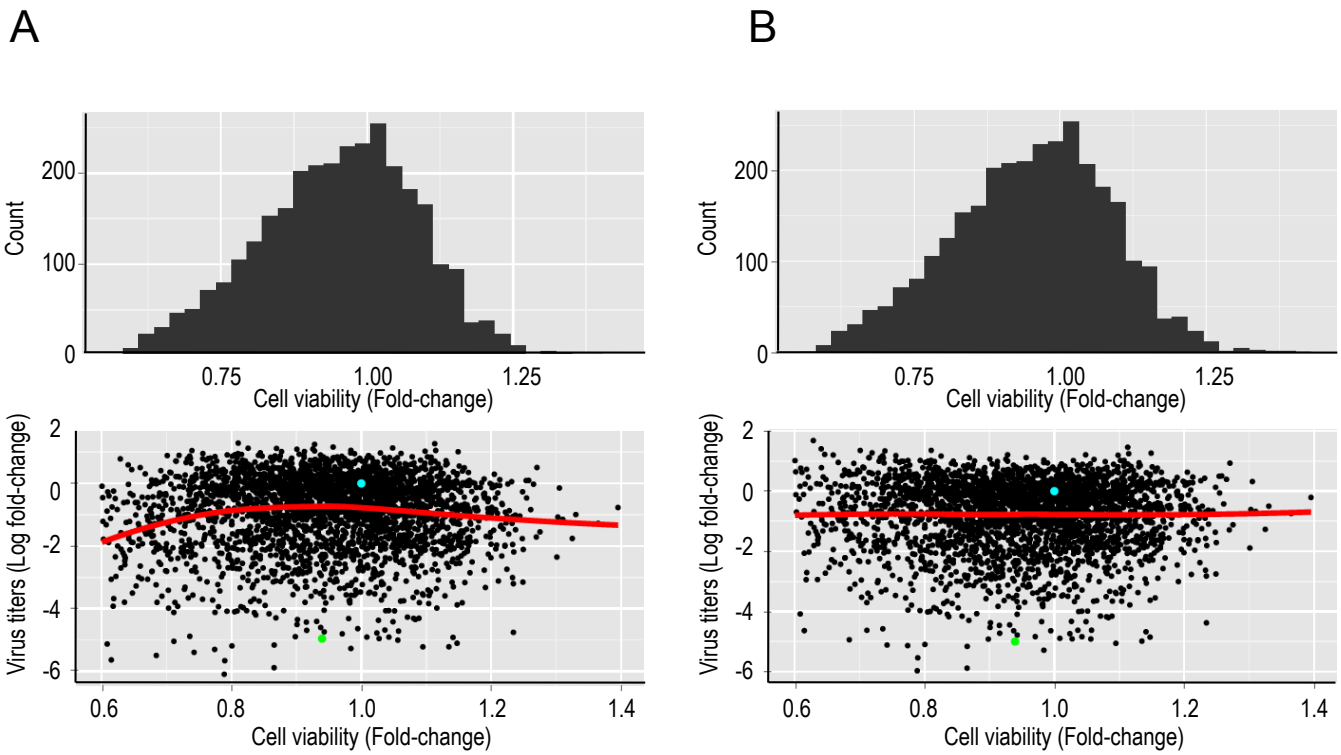

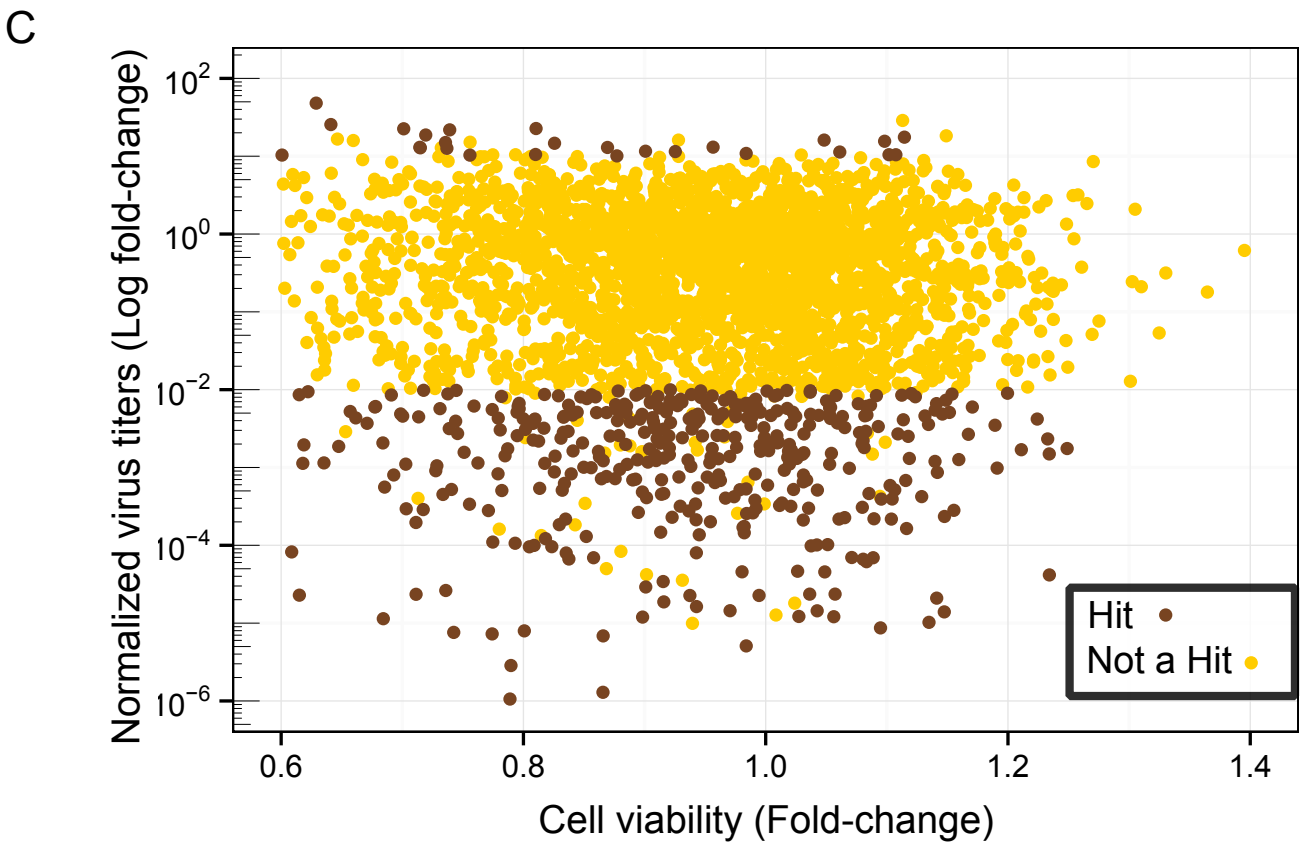

Fig. S1. Watanabe et al.

A

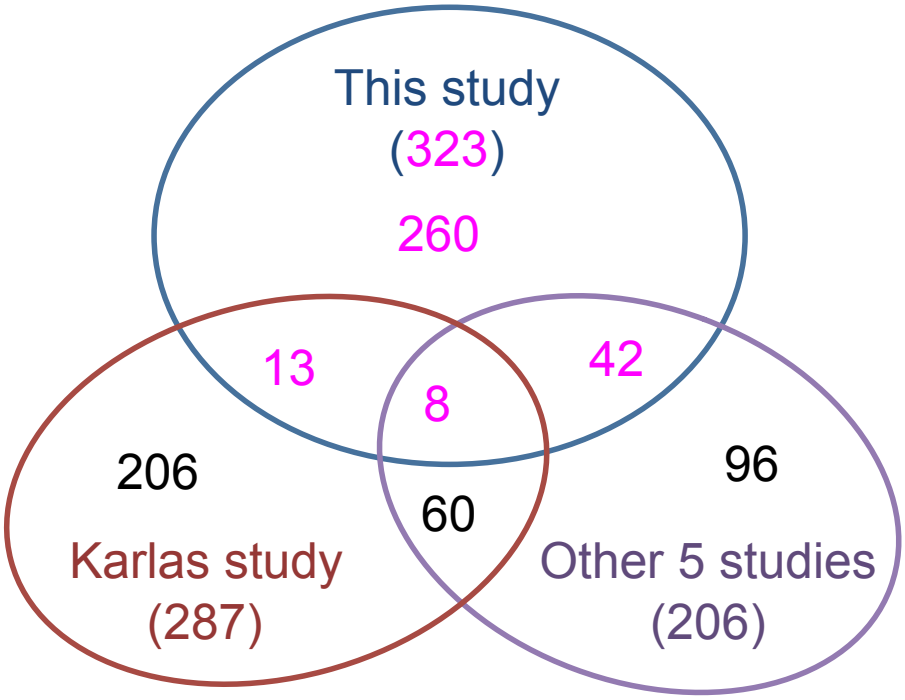

B

No. of host factors identified in this study that overlapped with other screens: (note that some of the factors detected in our study were found in more than one of the other studies)						
Karlas *et al*.	Konig *et al*.	Brass *et al*.	Shapira *et al*.	Hao *et al*.	Sui *et al*.	Total
21	12	15	16	15	3	63

Fig. S2. Watanabe et al.

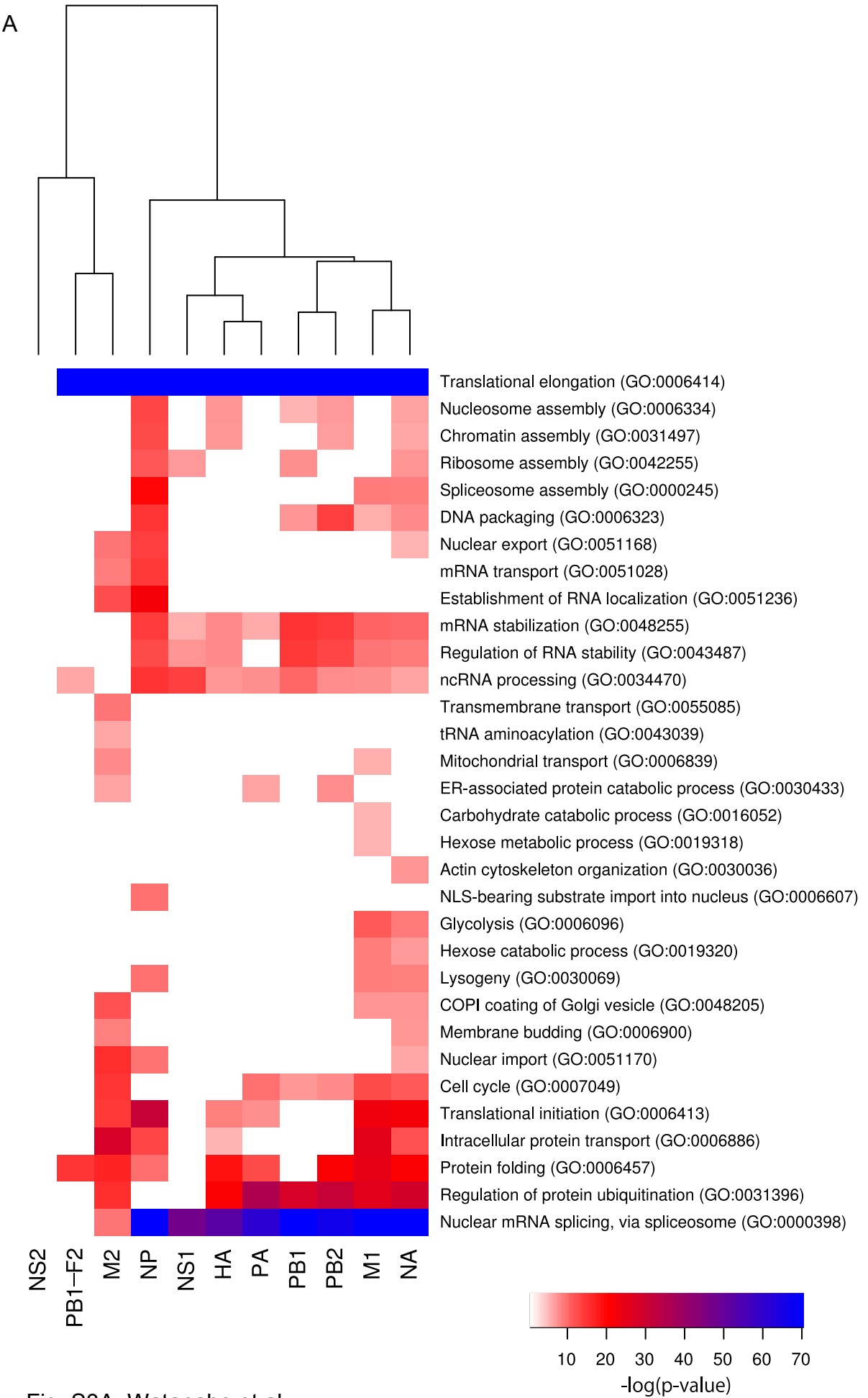

Fig. S3A. Watanabe et al.

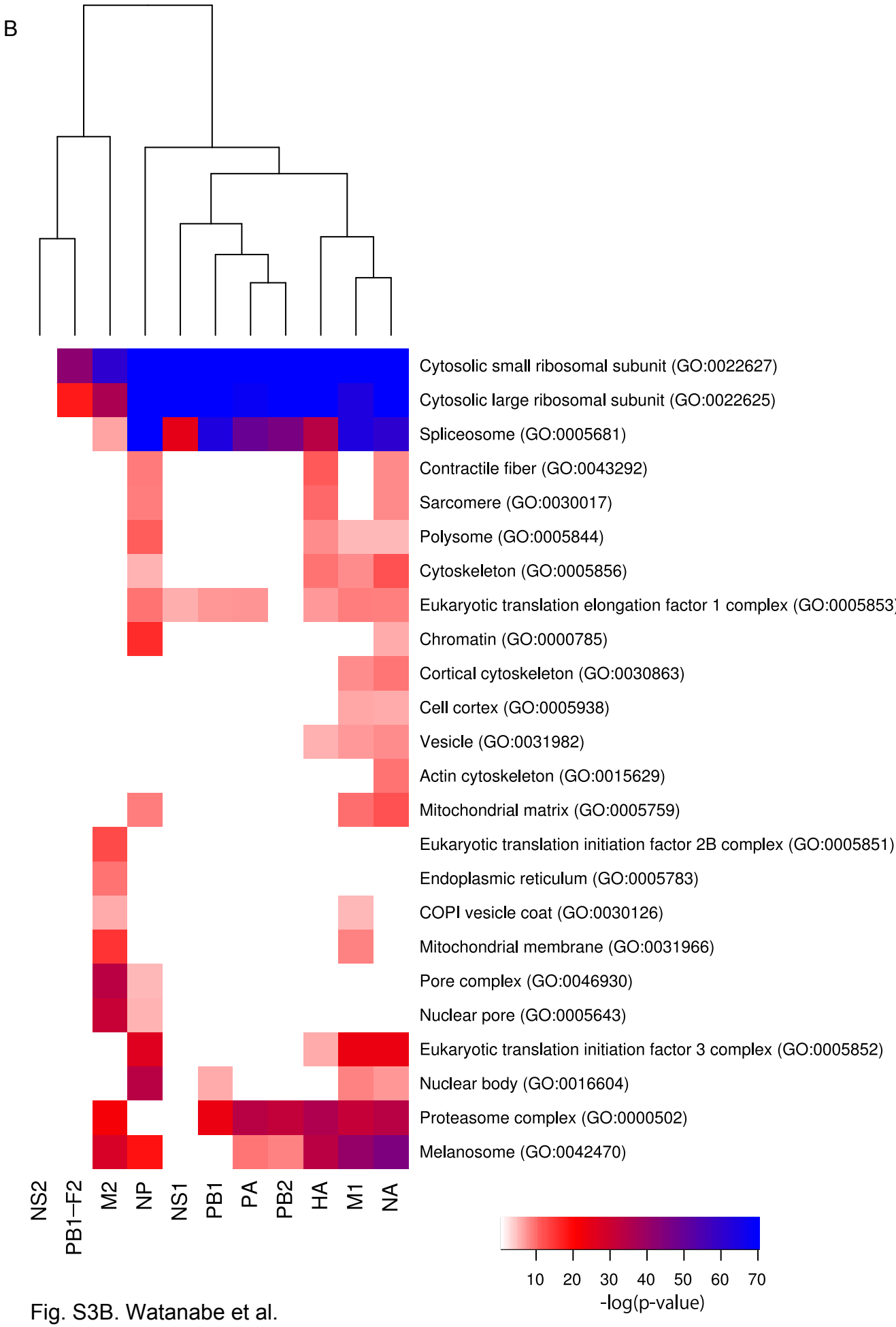

Fig. S3B. Watanabe et al.

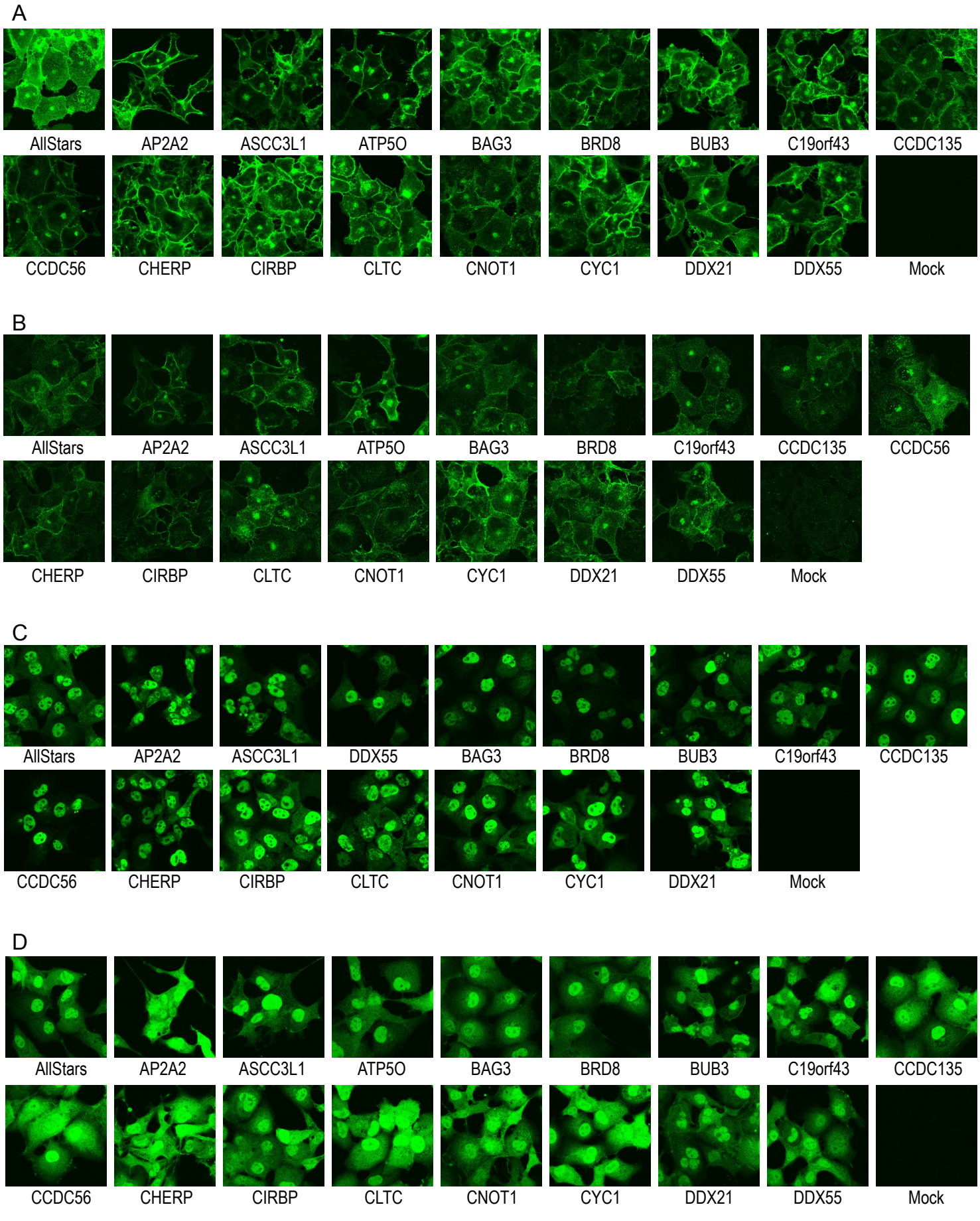

Fig S4. Watanabe et al.

A. Viral genome replication/transcription

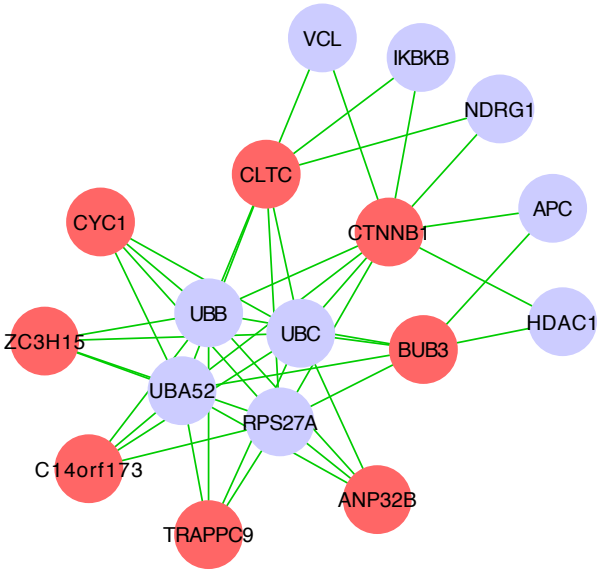

B. Early steps of viral life cycle

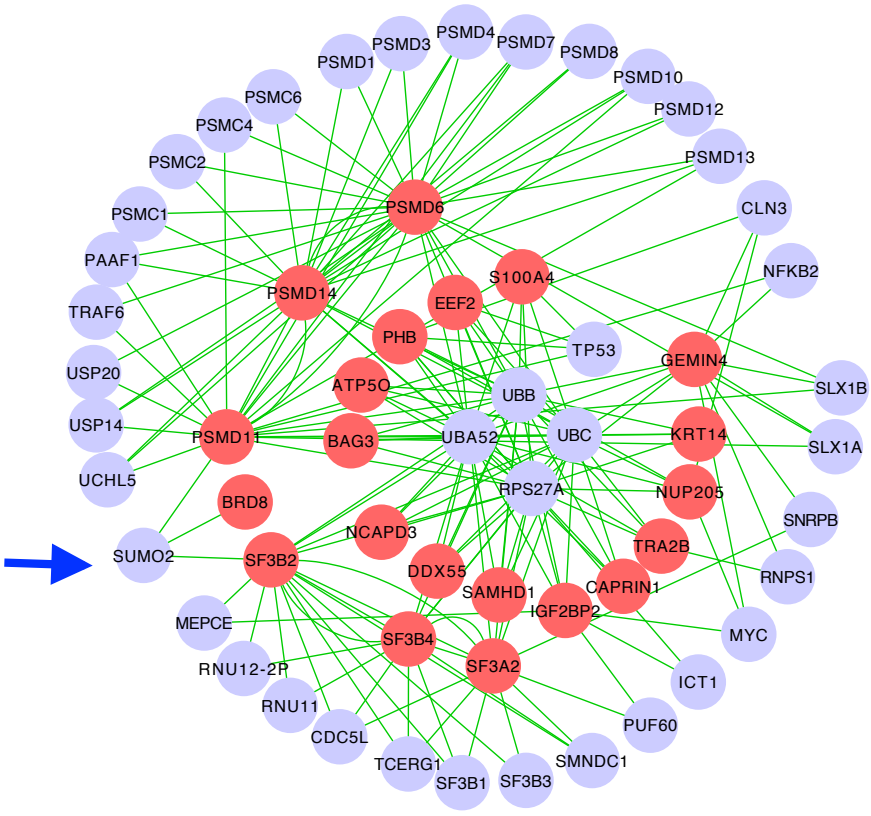

C. HA VLP formation

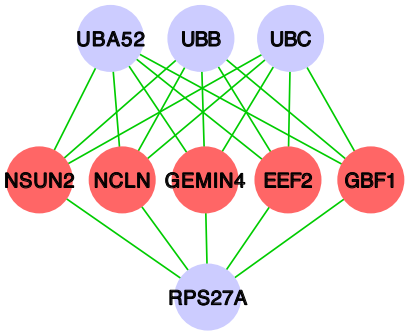

D. M1 VLP formation

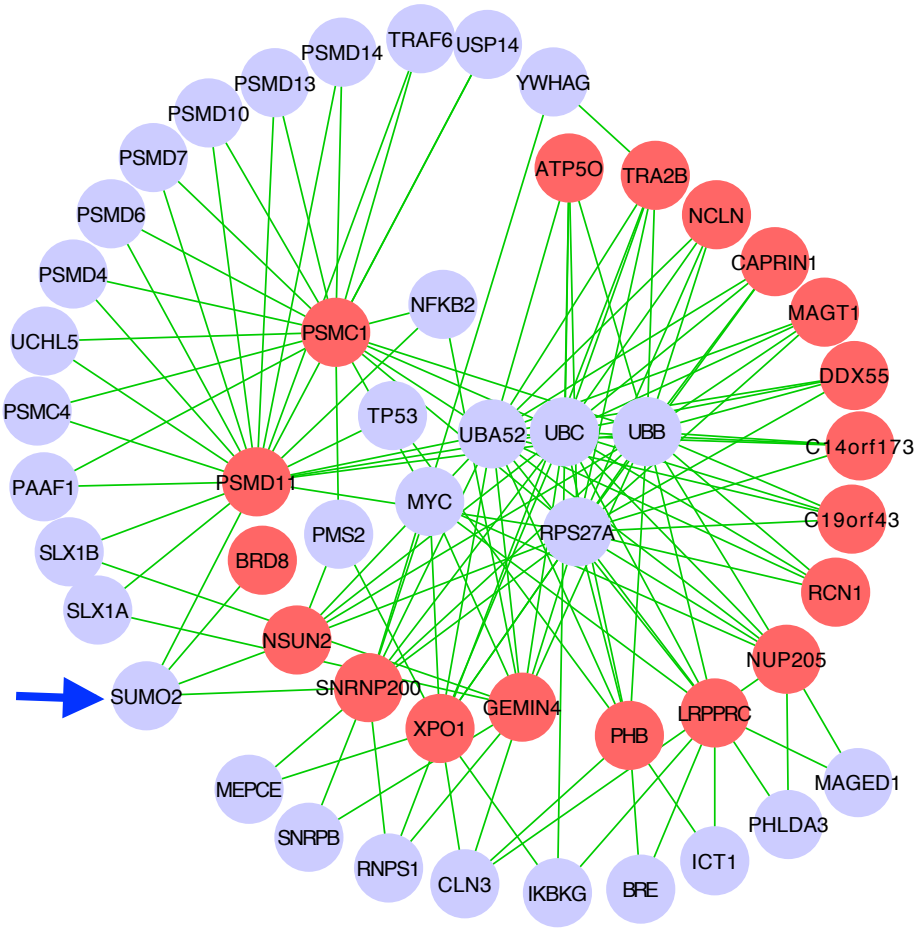

E. vRNP incorporation into virions

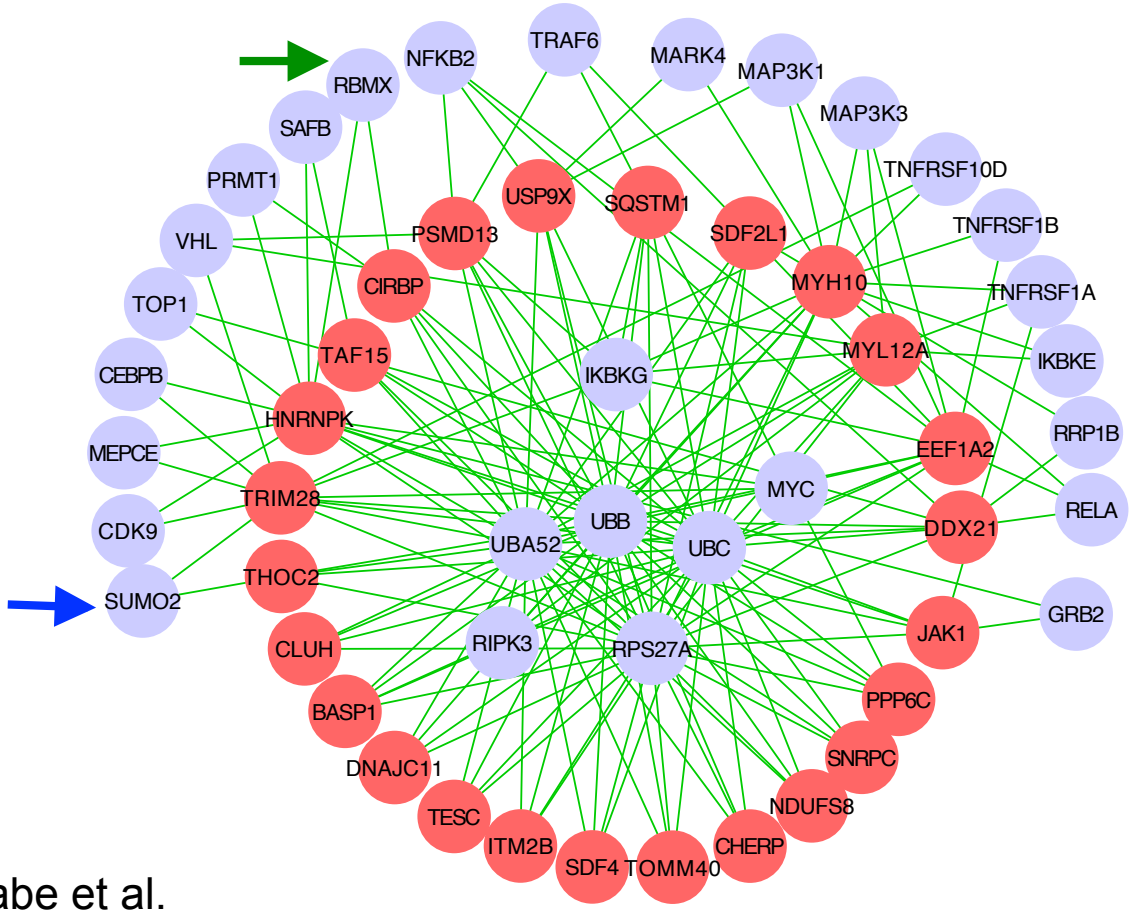

Fig. S5. Watanabe et al.

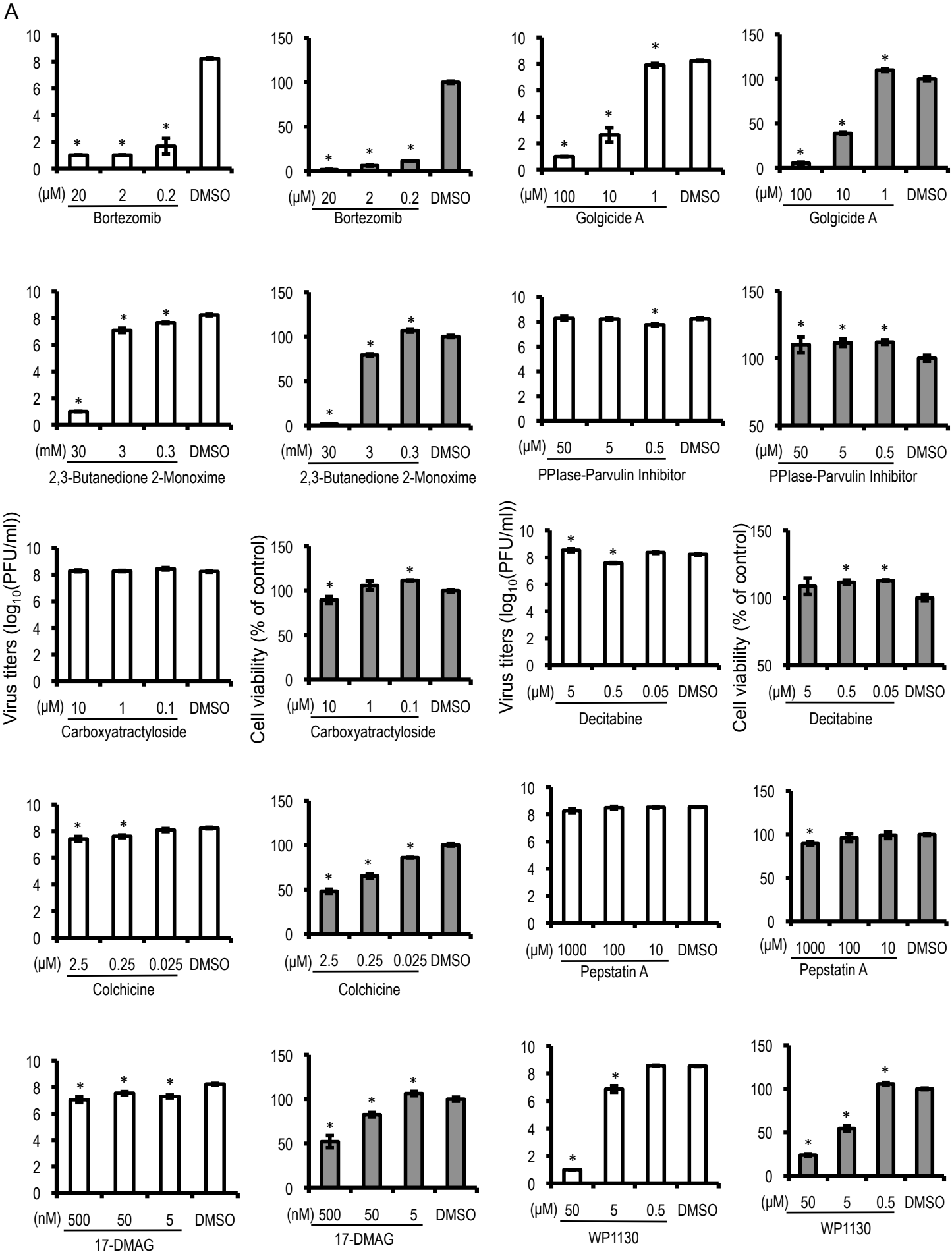

Fig. S6. Watanabe et al.

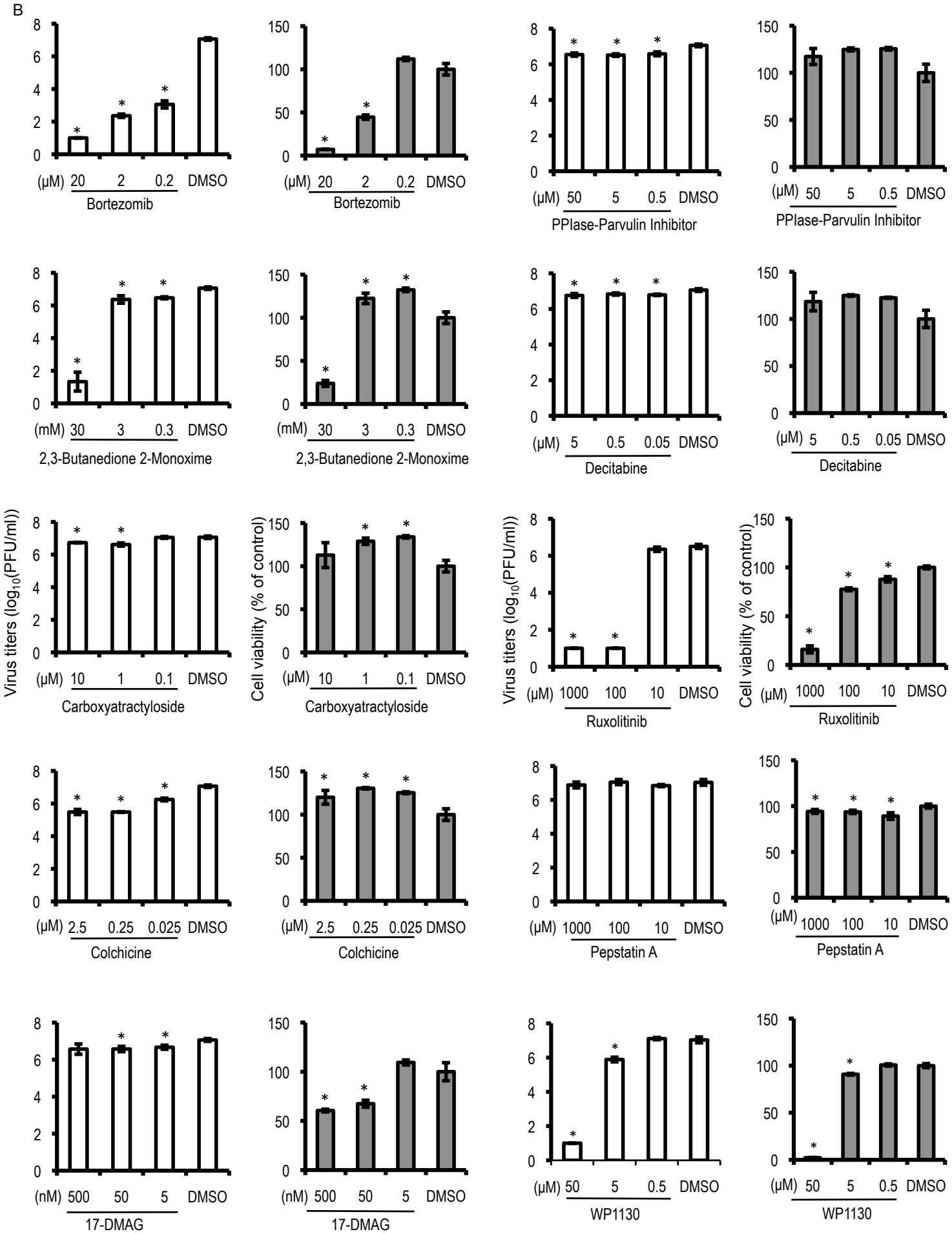

Fig. S6. Watanabe et al.

Supplemental Figure Legends

Figure S1, related to Figure 1. Identification of host genes whose siRNA-mediated down-regulation affected virus production. After removing all siRNAs that caused a fold-change (FC) in cell viability (relative to All Stars Negative Control) of 0.6 or greater, we applied LOESS normalization to remove additional cell viability-dependent effects in the virus growth data. (A) The distribution of the FC in cell viability for all siRNAs tested (top panel) and the dependence of the average virus titers on average cell viability in the raw data (lower panel). (B) Normalized data are shown. In (A) and (B), the cyan and green points highlight data corresponding to the negative and positive control siRNAs (i.e., AllStars Negative Control siRNA and siRNA against influenza virus NP gene, respectively), whereas the LOESS curve (red line) illustrates how the mean log-fold change (LFC) in virus titers fluctuated with cell viability before and after data normalization, respectively. (C) Scatter plot of the fold-change (FC) in normalized virus titers versus the FC in cell viability. 'Hit' (brown dot) indicates siRNAs that affected virus growth significantly ($p < 0.01$) (i.e., they reduced the normalized virus titers by more than 2-log units or increased them by more than 1-log unit compared with the negative control siRNA) without reducing cell viability by more than 40%. 'Not a Hit' (yellow dot) indicates that the respective siRNA had no significant effect on virus titers ($p > 0.01$), or that down-regulation of host gene expression by the respective siRNA could not be confirmed by qRT-PCR.

Figure S2, related to Figure 1. Comparison of the 323 genes identified in our study with the host genes identified in the six independent genome-wide screens for human genes involved in influenza virus replication. To determine whether any

of the genes identified in this study were also identified in previously reported genome-wide screens (Brass et al., 2009; Hao et al., 2008; Karlas et al., 2010; Konig et al., 2010; Shapira et al., 2009; Sui et al., 2009), we conducted pair-wise comparisons of our hits with those identified in previous genome-wide screens for human genes (including 110 *Drosophila* genes that have human orthologs) involved in influenza virus replication (Brass et al., 2009; Hao et al., 2008; Karlas et al., 2010; Konig et al., 2010; Shapira et al., 2009; Sui et al., 2009). (A) Venn diagram of the host factors identified as being involved in influenza virus replication in our study and in other studies. Shown are the total numbers of host genes whose suppression affected influenza virus replication (in parenthesis), and the numbers of host genes that were unique to the respective dataset or overlapped with the indicated dataset(s), respectively. (B) Numbers of host factors identified in this studies that overlapped with other studies. The dataset reported by Karlas *et al*. (Karlas et al., 2010) contains the highest number (21 genes) of host genes that were also identified by us, presumably because Karlas *et al.* used the same approach as we did (an RNAi-based screen in human cells) and the same influenza virus strain (i.e., WSN). By contrast, the screen by Sui *et al.* (Sui et al., 2009) identified the lowest number of host genes (3 genes) that were also identified by us, possibly due to differences in the screening systems used (RNAi screen vs. Random Homozygous Gene Perturbation library screen). See also Table S3.

Figure S3, related to Figure 1. Gene Ontology (GO) and pathway analyses of the 323 human genes identified to be involved in the influenza virus life cycle. Biological processes (A) and cellular components (B) in which the 323 human genes identified in this study are involved, based on DAVID (Huang et al., 2008) and

ConsensusPathBD (Kamburov et al., 2011). While most viral proteins interacted with a sufficient number of host proteins to perform an enrichment analysis and obtain significant results, the NS2 protein had too few binding proteins to perform this analysis. (A) The identified host factors are involved in various cellular functions, ranging from protein and RNA transport to cell cycle regulation as described in the main text. (B) Many of the identified host factors are involved in the formation of ribosomal complexes, eukaryotic translation elongation/initiation complexes, and proteasome complexes.

Figure S4, related to Figure 4. Effects of siRNAs targeting the 91 'top hits' on the intracellular localization of viral proteins in infected cells. To examine whether the down-regulation of the 91 'top hits' affects the intracellular localization of the viral proteins in virus-infected cells, siRNA-transfected HEK 293 cells were infected with 200 pfu of WSN virus per well of a 24-well tissue culture plate, fixed at 12 h post-infection, and then stained with anti-HA, anti-NA, anti-NP, or anti-M1 antibody. Intracellular localization of HA (A), NA (B), NP (C), and M1 (D) are shown in Figure 4 and Figure S4. Because all of the pictures were taken under the same conditions, some were overexposed, and therefore, it was difficult to determine whether some of the host factors are involved in the localization of viral proteins. However, siRNAs targeting *SFRS10*, *GBF1*, *KRT14*, *CAPRIN1*, and *PPP6C* clearly altered the localization of HA (Figure 4A), whereas those targeting *PPP6C*, *BUB3*, *GBF1*, *KRT14*, and *SDF2L1* affected NA localization (Figure 4B). Our results suggest that these host proteins may be involved in the transport of HA, NA, or both to the plasma membrane. In the presence of siRNAs against *PHB*, *ITGB4BP*, *PSMD11*, *VCP*, *XPO1* or *ATP5O*, NP accumulated in the nucleus, whereas it localized to the nucleus and

cytoplasm in control cells (Figure 4C). The host factors that affected NP localization also reduced cellular transcription/translation, with the exception of *XPO1* (also known as *CRM1*), which mediates influenza vRNP nuclear export through an interaction with the viral nuclear export protein (NS2=NEP) (Boulo et al., 2007; Elton et al., 2001; Neumann et al., 2000). By contrast, none of the siRNAs shown in Figure S4 had an appreciable effect on the localization of the viral proteins (representative images are shown). The same images for AllStars controls are also used in Figures 4A–C as a reference.

Figure S5, related to Figures 2 and 3. Interaction networks of host proteins that affect different steps of the influenza virus life cycle. (A–E) Depicted are host factors that are potentially involved in the indicated step(s) of the influenza viral life cycle (red circle) and share cellular binding partners (purple circle) with at least one other 'red' host factors (note that these criteria led to the exclusion of some of the factors described in the text). The interaction networks are visualized by using Cytoscape (http://cytoscape.org/). (A) Viral genome replication/transcription. CCDC56 (Table S5A) was excluded based on the criteria described above. TRAPPC9 is an alternate name for NIBP. (B) Early steps of the viral life cycle. DPM3 and CCDC135 (Table S5A) were excluded based on the criteria described above. TRA2B is an alternate name for SFRS10. (C, D) HA and M1 VLP formation. DPM3 (Table S5A) was excluded based on the criteria described above. SNRNP200, MAGT1, and NSUN2 are alternate names for ASCC3L1, DKFZp564K142, and FLJ20303, respectively. (E) vRNP incorporation into virions. RPL26, SFRS28, and PCDHB12 (Table S5A) were excluded based on the criteria described above. CLUH and MYL12A are alternate names for KIAA0664 and MRCL3, respectively. Blue and

115 green arrows indicate SUMO2 and RBMX, respectively, which are discussed in the
116 text.
117
118 **Figure S6, related to Figure 6. Effects of selected drugs on virus titers and cell**
119 **viability in virus-infected cells.** HEK 293 or A549 cells were infected with WSN
120 virus at an MOI of 0.001. After incubation for one hour, cells were washed and
121 incubated with medium containing the indicated concentration of drugs. DMSO (final
122 concentration, 1%) was `used as a control. Forty-eight hours later, culture
123 supernatants were harvested for virus titration and cell viability was determined by
124 using CellTiter-Glo. (A and B) Drugs targeting host factors identified in our siRNA-
125 based screen were tested in HEK 293 (A) or A549 (B) cells. Averages and standard
126 deviations of 3 replicates are shown. The *p* value was calculated with Welch's t-test
127 compared with a non-targeting siRNA control. To control for the multiplicity effect, *p*
128 values were adjusted using Benjamini-Hochberg's procedure keeping the false
129 discovery ratio < 0.05. Asterisk indicates that the adjusted *p* value is < 0.05.
130

Supplemental Experimental Procedures

Pull-down assay and mass spectrometry. HEK 293 cells were transfected with a plasmid encoding an N- or C-terminally FLAG-tagged influenza viral protein by using TransIT 293 reagent (Mirus Bio Corp., Madison, WI, USA). After 24 h, the cells were lysed with lysis buffer [50 mM Tris-HCl (pH 7.5), 150 mM NaCl, 1 mM EDTA, 0.5% Nonidet P-40, and protease inhibitor mixture Complete Mini (Roche, Mannheim, Germany)] for 1 h at 4 °C. After centrifugation, the supernatants were incubated with an anti-FLAG M2 Affinity Gel (Sigma-Aldrich) for 18 h at 4 °C. The affinity gel was then washed three times with lysis buffer and twice with immunoprecipitation (IP) buffer [50 mM Tris-HCl (pH 7.5), 150 mM NaCl, and 1 mM EDTA]. Proteins were eluted for 2 h with IP buffer containing 0.5 mg/mL FLAG peptide (Sigma-Aldrich) at 4 °C with agitation. The affinity gel was removed by centrifugation, and the supernatants were then filtered through an Ultrafree-MC filter (Millipore). The eluted proteins were then subjected to nanoflow liquid chromatography tandem mass spectrometry (nanoLC-MS/MS) analysis. Q-STAR Elite (AB SCIEX) coupled with Dina (KYA Technologies) was used to analyze the mass spectrometry data. Co-immunoprecipitated host proteins were identified by comparing MS/MS signals with the RefSeq (National Center for Biotechnology Information) human protein database (38,946 sequences as of April 7, 2009) and by using the Mascot algorithm (version 2.2.04; Matrix Science) with the following parameters: variable modifications, oxidation (Met), N-acetylation; maximum missed cleavages, 2; peptide mass tolerance, 200 ppm; and MS/MS tolerance, 0.5 Da. Protein identification required at least one MS/MS data signal with a Mascot score that exceeded the threshold ($p < 0.05$).

Protein-protein interaction analysis.

We used HIPPIE database v1.4 (Schaefer et al., 2012) to analyze the interaction of host factors involved in one or more steps of influenza replication with other human proteins (Supplementary Table S5E–J). We started filtering the HIPPIE database by removing all interactions with a quality score ≤ 0.7. Next, similar to a previous study (Tu et al., 2009), we pruned the original database by leaving only proteins that interacted with at least two host factors whose down-regulation affected influenza virus titers (Supplementary Figure S5) – this provided insights into the mechanisms involved in the different steps of the influenza replication cycle. In all network analyses, the HIPPIE database was converted to an undirected graph and processed using R (version 2.10.1) and the iGraph library (version 0.5.4).

Gene Ontology and pathway analyses for the 323 host factors that co-immunoprecipitated with viral proteins and affected virus titers in cultured cells.

For the set of 323 host factors that co-immunoprecipitated with viral proteins and affected influenza virus replication, major gene functions were determined. Our Gene Ontology (GO) and pathway analyses based on two web-resources, DAVID (Huang et al., 2008) and ConsensusPathBD (Kamburov et al., 2011), revealed that the identified host factors are involved in various cellular functions, ranging from protein and RNA transport to cell cycle regulation (Table S4). Most influenza viral proteins co-immunoprecipitated with host proteins involved in transcription, translation, mRNA splicing mechanisms, and proteasome complexes (Table S4). In addition, some viral proteins co-immunoprecipitated with host factors that are involved in specific cellular functions. For example, some of the M1- and NA-binding partners

180 are involved in glycolysis and COPI-coating of Golgi vesicles, and some of the NP-
181 binding partners function in protein import and export to the nucleus (Table S4B).
182
183 **Immunofluorescence microscopy.** HEK 293 cells transfected with the respective
184 siRNAs were infected with WSN virus. At 12 h after influenza virus infection, HEK
185 293 cells were fixed with 4% paraformaldehyde in phosphate buffer (4% PFA/PB) for
186 10 min, and then permeabilized by using 0.05% Triton-X100 in 4% PFA/PB for 10
187 min. The cells were then blocked with Blocking One solution (Nacalai Tesque, Kyoto,
188 Japan) for 30 min. To detect viral proteins, the cells were incubated overnight at 4 °C
189 with anti-HA (WS3-54), anti-NA (WS5-29), anti-NP (Aichi347/4), or anti-M1
190 (WS27-52) antibody diluted in Blocking One solution. After three washes with PBS
191 containing 0.05% Tween-20 (v/v) (PBST), the cells were incubated for 2 h with Alexa
192 Fluor 488 goat anti-mouse IgG (Molecular Probes) diluted in 10% Blocking
193 One/PBST. Fluorescence signals were observed under a confocal laser microscope
194 (LSM510META; Carl Zeiss, Jena, Germany).
195
196 **Western blotting.** Proteins on SDS-PAGE gels were transferred to a PVDF
197 membrane for 1 h at 15 V, and the membrane was then incubated with a saturating
198 volume of Blocking One solution (Nacalai Tesque) for 30 min at room temperature or
199 for 18 h at 4 ºC. Then, the membrane was incubated for at least 1 h at room
200 temperature with anti-WSN (R309) or anti-β-actin (AC-74) antibody diluted in
201 solution I of Can Get Signal (TOYOBO). The membrane was then washed three times
202 with TBS supplemented with 0.05% (v/v) Tween-20 (TBST), and incubated with
203 ECL anti-mouse IgG, horseradish peroxidase-linked whole antibody (from sheep; GE
204 Healthcare) or ECL anti-rabbit IgG, horseradish peroxidase-linked whole antibody

(from donkey; GE Healthcare) diluted in solution II of Can Get Signal (TOYOBO). After being washed three times with TBST, the membrane was incubated with ECL Prime Western blotting detection reagent (GE Healthcare), and chemiluminescence signals were visualized by means of a VersaDoc Imaging System (Bio-Rad).

Supplemental References

Schaefer, M.H., Fontaine, J.F., Vinayagam, A., Porras, P., Wanker, E.E., and Andrade-Navarro, M.A. (2012). HIPPIE: Integrating protein interaction networks with experiment based quality scores. PLoS One *7*, e31826.

Tu, Z., Argmann, C., Wong, K.K., Mitnaul, L.J., Edwards, S., Sach, I.C., Zhu, J., and Schadt, E.E. (2009). Integrating siRNA and protein–protein interaction data to identify an expanded insulin signaling network. Genome Research *19*, 1057-1067.